IJARSCT
ISSN (Online) 2581-9429
International Journal of Advanced Research in Science, Communication and Technology (IJARSCT)
Volume 11, Issue 1, November 2021
Impact Factor: 5.731

Preparation of Nanostructured SnO_2-NiO Composite Semiconductor for Gas Sensor Applications

S. Kumar[1], P. Gowthaman[2], J. Deenathayalan[3]
Assistant Professor, Department of Electronics, Sri Vasavi College, Erode, Tamilnadu, India[1]
Assistant Professor, Department of Electronics, Erode Arts and Science College, Erode, Tamilnadu, India[2]
Principal, Gandhi Arts and Science College, Sathyamangalam, Tamilnadu, India.[3]
Corresponding Author Email: yeskumar.com@gmail.com[1]

Abstract: *Electro spinning technology combined with chemical precipitation method and high-temperature calcination was used to prepare SnO_2-NiO composite semiconductor nanofibers with different Sn content. Scanning electron microscope (SEM), X-ray diffractometer (XRD) and energy dispersive X-ray spectrometer (EDS) were used to characterize the morphology, structure and content of various elements of the sample. Using ethanol as the target gas, the gas sensing properties of SnO_2-NiO nanofibers and the influence of Sn content on the gas sensing properties of composite nanofibers were explored. The research results show that SnO_2-NiO composite nanofibers have a three-dimensional network structure, and the SnO_2 composite can significantly enhance the gas sensitivity of NiO nanofibers. With increase of SnO_2 content, the response sensitivity of composite fibers to ethanol gas increases, and the response sensitivity of composite nanofibers with the highest response to ethanol gas with a volume fraction of 100×10^{-6} at the optimal working temperature of 160□ are13.4;It is 8.38 times the maximum response sensitivity of NiO nanofibers. Compared with the common ethanol gas sensor MQ-3 on the market, SnO_2-NiO composite nanofibers have a lower optimal working temperature and higher response sensitivity, which has certain practical application value.*

Keywords: Tin Dioxide; Nickel Oxide; Nanostructured Semiconductor; Gas Sensor; Composite Materials.

I. INTRODUCTION

A gas sensor is a device that is sensitive to gas composition and concentration and can convert gas data into electrical signals for detection [1]. It has the characteristics of convenient operation, fast response speed, miniaturization of equipment and low cost. It is used in the field of gas detection and monitoring. It has broad development space and application prospects [2, 3, 4, 5]. Ethanol (C_2H_5OH) is the most common monohydric alcohol and an important industrial raw material, widely used in the fields of biochemistry, food, transportation and medical safety. Ethanol is flammable and volatile at room temperature, and prolonged exposure to ethanol vapor may have adverse effects on human health, such as sensory stimulation, liver damage, and damage to the central nervous system [6, 7, 8]. Therefore, it is of great practical significance to use gas sensors to monitor ethanol gas in real time in industrial production and medical research. MQ-3 is a sensitive element in the ethanol gas sensor widely used in the market. The sensitive material is mainly tin dioxide (SnO_2), which belongs to a metal oxide semiconductor (MOS) gas sensor [9]. MQ-3 has high response sensitivity to ethanol gas, and can work normally in the environment of water vapor, flue gas and other gases, and the detection concentration range of ethanol gas is very wide, the price is low, and it is a gas with high cost performance. Sensors are widely used in motor vehicle drivers and some workplaces where work after drinking is strictly prohibited [10].

However, SnO_2 gas-sensing materials still have the defect of high working temperature (about 300□) in the gas sensing process [11]. High temperature will cause the thermal growth of metal oxides, resulting in decreased sensor stability and shorter life span. When detecting flammable and explosive gases, gas sensors in high temperature environments may also cause deflagration and become a safety hazard [12]. At the same time, a higher operating

IJARSCT
ISSN (Online) 2581-9429
International Journal of Advanced Research in Science, Communication and Technology (IJARSCT)
Volume 11, Issue 1, November 2021
Impact Factor: 5.731

temperature consumes more energy and the device structure is more complicated. Therefore, the currently widely used ethanol gas sensor still has a lot of room for improvement in the working performance.MOS gas-sensitive materials have the advantages of low raw material cost, environmental friendliness, simple preparation process, good stability, long life and controllable structure [13, 14, 15]. Common MOS gas sensing materials include zinc oxide [16], tin oxide [17], titanium dioxide [18], iron oxide [19] and nickel oxide [20], among which nickel oxide is a typical wide band gap p -Type semiconductor material with good gas sensitivity. As a gas-sensitive material, nickel oxide has the advantages of good chemical stability, high catalytic activity, and little influence on humidity [21]. Tin oxide has an oxygen-deficient structure and exhibits n-type semiconductor characteristics. As a gas-sensitive material, it has the characteristics of fast absorption and desorption and a wide range of applicable gases [22]. By constructing heterostructures of n-type and p-type semiconductor materials, the gas sensitivity of the materials can be further improved.

For example, Li et al. [23] used a uniform electrospinning method and a heat treatment method to prepare a new cage structure α -Fe_2O_3 /SnO_2 composite nanofibers, the results show that the cage nanofibers have high selectivity to acetone, and the response recovery time to 100 mg/L acetone reaches 1.5 and 2.5 s, respectively. Jayababu et al. [24] prepared NiO semi-shielded SnO_2(NiO- SnO_2) nanocomposites by co-precipitation and sol-gel methods . The test results showed that NiO/ SnO_2 responds to 100 mg/L ethanol at room temperature It is 140, which is 9 times higher than SnO_2 sensor and 11 times higher than NiO sensor. Wei et al. [25] prepared a nanocomposite with SnO_2nano-needles anchored on the surface of NiO microspheres by hydrothermal method combined with heat treatment. The results showed that SnO_2-NiO was at the optimal working temperature (230□) mg of 20 is / L NO_2 response is 14.45, while the original NiO at the optimal operating temperature (320 □) of NO 2 in response to 3.03, while of SnO_2-NiO in the NO 2 content of ~ 50 cm & lt. $1.^3$ / $m^{At\ 3}$ o'clock, the response value shows a very good linear relationship with the concentration.

Among various nanostructures, one-dimensional nanomaterials are not limited by the nanoscale in length, and can conduct electrons, photons, etc. quickly, thereby improving the characteristics of the material in terms of electronic transmission and mechanical properties. Therefore, in addition to all the superior properties of nanomaterials, one-dimensional nanostructures also have excellent thermal stability, optical properties, photoelectric conductivity, and mechanical properties, making them a hot material in the field of sensor research [26]. At present, there are many methods for preparing one-dimensional nanomaterials. The most typical ones are: laser sputtering method [27], arc discharge method [28], template method [29], chemical vapor deposition method [30] and electro spinning method [31] etc. Among the many nanomaterial preparation technologies, electrospinning (Electrospinning) is easy to operate and low in cost, and it is an efficient method for preparing nanofibers [32]. However, when preparing inorganic nanofibers, the electrospinning technology still has certain limitations in terms of the flexibility of fiber microstructure control and the uniformity of the dispersion of inorganic particles in the fiber. Therefore, it is an effective way to develop high-performance MOS gas-sensing materials by combining electrospinning technology with chemical preparation methods and adjusting the microscopic morphology, structure and composition of fibers to achieve the improvement of nanofiber material performance.

In this study, electrospinning technology combined with chemical precipitation and high temperature heat treatment was used to prepare SnO_2-NiO composite semiconductor nanofibers, and the relative content of Sn and Ni elements in the composite fibers was adjusted. By testing the gas sensing performance, the sensitivity of SnO_2-NiO composite nanofibers to ethanol gas was explored, the influence of Sn content on the gas sensitivity of composite fibers was analyzed, and the gas sensing mechanism of composite fibers was discussed.

II. Experimental Method

2.1 Raw Materials

Polyacrylonitrile (PAN, average M w=1.5×10^5), analytical grade, Bailingwei Technology Co., Ltd.; N , N -dimethylformamide (DMF) and absolute ethanol, both analytical grade, Tianjin Branch Ou Chemical Reagent Co., Ltd.; Ammonia, analytical grade, Tianjin Fuyu Fine Chemical Co., Ltd.; $NiSO_4 \cdot 6H_2O$ and $SnCl_4 \cdot 5H_2O$, both

IJARSCT
ISSN (Online) 2581-9429
International Journal of Advanced Research in Science, Communication and Technology (IJARSCT)
Volume 11, Issue 1, November 2021
Impact Factor: 5.731

analytical grade, Sinopharm Chemical Reagent Co., Ltd. The experimental water is deionized water, and the chemicals involved in the experiment are all analytically pure.

2.2 Synthetic Sample

Preparation of one-dimensional carbon nanofibers (CNFs) template: 0.8 g PAN was added to 10 mL DMF and stirred at room temperature for 12 h to form a transparent spinning precursor solution with a certain viscosity. The precursor solution was placed in a 10 mL syringe with a stainless steel needle, the inner diameter of the needle was 0.8 mm, the syringe advancement speed was set to 0.8 mL/h, and the distance and voltage between the receiving device and the needle were 15 cm and 12 kV, respectively. Dry the white PAN film obtained by spinning at 60 □ to remove the incompletely evaporated solvent, put the dried PAN into a tube furnace for heat treatment, first heat it up to 270 □ in the air at a heating rate of 2 □/min. Insulate for 2 h, then under the protection of nitrogen (N_2), the temperature is increased to 800 □ at a heating rate of 5 □/min, and the temperature is kept for 1 h and then cooled in the furnace. The obtained sample is carbon nanofiber, which is used as one-dimensional preparation of composite nanofibers template.Preparation of SnO_2-NiO composite semiconductor nanofibers: Dissolve 0.02 mol $NiSO_4 \cdot 6H_2O$ in 90 mL deionized water to obtain a $NiSO_4$ aqueous solution. The CNFs film was immersed in a $NiSO_4$ aqueous solution, and 3 mL of ammonia (ammonia concentration was 13.38 mol/L) was added dropwise under magnetic stirring. After standing for 20 minutes at room temperature, it was taken out and washed with deionized water several times. Air-dried for 30 min to obtain CNFs loaded with $Ni(OH)_2$, denoted as CNFs@$Ni(OH)_2$.CNFs@$Ni(OH)_2$ was heat-treated in a 600□ tube furnace for 4 h (heating rate is 1□/min, air atmosphere) to obtain nickel oxide nanofibers (NiO NFs) as a control sample.

The molar ratios of $SnCl_4 \cdot 5H_2O$ and $NiSO_4 \cdot 6H_2O$ are 1:100, 1:20, 1:5 and 1:1 to prepare different concentrations (2.22, 11.1, 44.4 and 222 mmol/L). $SnCl_4$ aqueous solution. At room temperature,immerse CNFs@$Ni(OH)_2$ in the above four sets of $SnCl_4$ solutions and let stand for 20 min, then take them out and wash them with deionized water 3 times to obtain $Sn(OH)_4$CNFs@$Ni(OH)_2$. The samples collected from 2.22, 11.1, 44.4, and 222 mmol/L $SnCl_4$ solutions are respectively labeled asCNFs@$Ni(OH)_2$ /$Sn(OH)_4$ -1,CNFs@$Ni(OH)_2$ /$Sn(OH)_4$ -2, CNFs@$Ni(OH)_2$ /$Sn(OH)_4$ -3 and CNFs@$Ni(OH)_2$ /$Sn(OH)_4$ -4. The four groups of samples were placed in a 600□ tube furnace, and heated in the air at a heating rate of 1 □/min and kept for 4 h. The carbon fiber is completely decomposed, and at the same time, $Sn(OH)_4$ and $Ni(OH)_2$ are converted into SnO_2 and NiO, and SnO_2-NiO composite nanofibers are obtained, which are respectively denoted as SnO_2 -NiO-1, SnO_2 -NiO-2, SnO_2 -NiO-3 and SnO_2 -NiO-4NFs. This mechanism works as prepared in Fig 1.

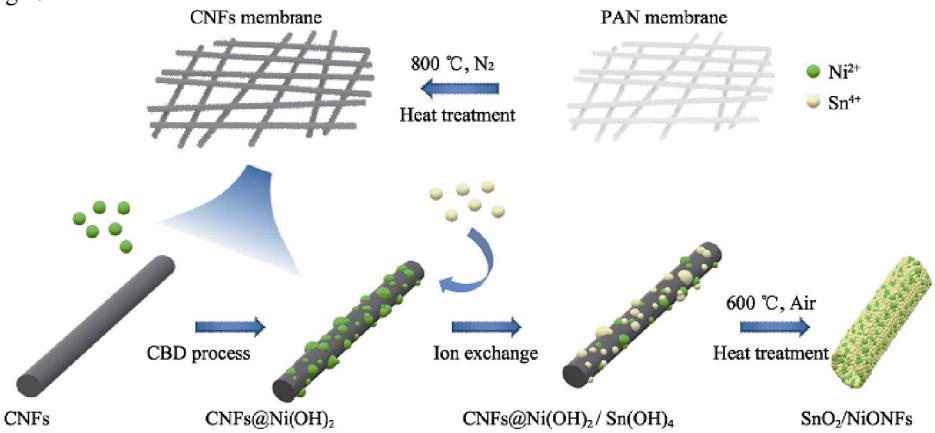

Figure 1: Preparation mechanism diagram of SnO 2 /NiO NFs

IJARSCT
ISSN (Online) 2581-9429
International Journal of Advanced Research in Science, Communication and Technology (IJARSCT)
Volume 11, Issue 1, November 2021
Impact Factor: 5.731

2.3 Characterization Method

The JSM-7800F field emission scanning electron microscope of JEOL was used to analyse the microscopic morphology and structure of SnO_2-NiO nanofibers; Shimadzu's XRD-7000S X-ray diffractometer (XRD, D/max3B, Cu-K) was used. α radiation, λ =0.154nm) analyse the crystal structure of composite nanofibers; use Oxford Instruments' X-Max50 energy spectrometer to analyse the element type and content of the sample.

2.4 Testing Method

Use the WS-30A gas sensitivity tester (Zhengzhou Weisheng Electronic Technology Co., Ltd.) to test the gas sensitivity performance of the sample. The test system is mainly composed of an information acquisition system and a test box. The test box is a closed space with a volume of 18 L. There are built-in heating plates, fans and load resistors. The gas sensor is composed of a ceramic tube and a Ni-Cr heating wire inserted into the ceramic tube. The test sample is mixed with absolute ethanol to form viscous slurry, and then the surface of the ceramic tube is coated, and the coated gas sensor is heated at 160 □ for 48 h to age the element and improve the stability of the element. The response value of the sensor $S = R_a / R_g$, where R a and R g are the resistance of the sensor in air and test gas, respectively.

III. Results and Discussion

3.1 Morphology and Structural Characteristics

Figure 2 (a) is the SEM photo of CNFs@$Ni(OH)_2$ nanofibers. It can be seen from the figure that the sample generally has a fiber morphology, and the fibers are randomly distributed to form a three-dimensional network structure; the nanofibers are continuous and uniform in diameter. The average diameter is about 300 nm; many nanoparticles grow randomly and uniformly on the surface of the fiber. CBD) $Ni(OH)_2$ produced . During the chemical precipitation reaction, the ammonia water reacts with Ni^{2+} in the $NiSO_4$ aqueous solution to generate the amine complex ion $Ni(NH_3)_6^{2+}$, and the reaction is as shown in formula (1). With the slow release of hydroxide ions in the aqueous ammonia solution, this complex ion cannot exist stably, and reacts with hydroxide to form a more stable nickel hydroxide precipitate. The reaction is as shown in formula (2) [33].

$$Ni^{2}++6NH_3\cdot H_2O \rightarrow Ni(NH_3)_6^{2+}+6H_2O \quad (1)$$

$$Ni(NH_3)_6^{2+}+2OH-+6H_2O \rightarrow Ni(OH)_2+6NH_3\cdot H_2O \quad (2)$$

The produced $Ni(OH)_2$ is adsorbed on the surface of CNFs to form nucleation to obtain lower nucleation work. As the reaction progresses to the right side of the reaction formula, more $Ni(OH)_2$ is generated and grows along the $Ni(OH)_2$ nucleus originally adsorbed on the surface of CNFs until the reaction reaches equilibrium [34 , 35] . Figure 2 (b) is the SEM photo of NiO NFs obtained after CNFs@$Ni(OH)_2$ heat treatment at 600 □. After the heat treatment, the hydroxide $Ni(OH)_2$ is converted to the oxide NiO, and the CNFs decomposes into small molecules such as CO_2 and escapes under high temperature in the air atmosphere , forming nanofibers with a hollow structure. NiO hollow nanofibers are composed of NiO particles, and the diameter shrinks to about 200 nm after heat treatment.

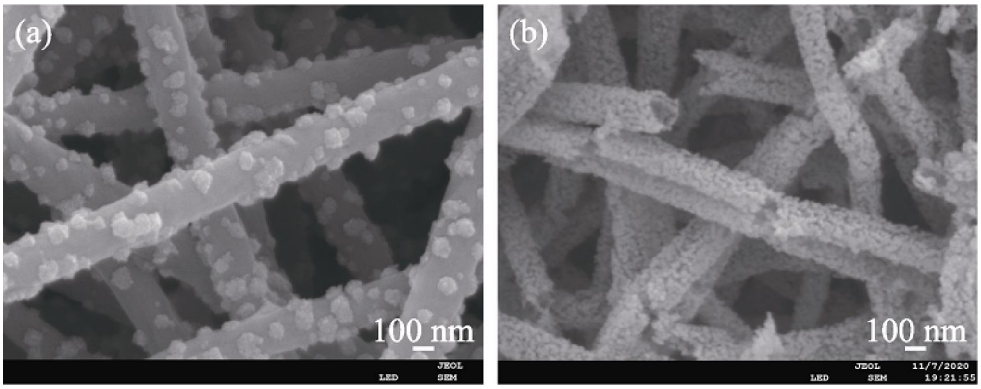

Figure 2: SEM images of **(a)** CNFs@$Ni(OH)_2$ and **(b)**NiO NFs

IJARSCT
ISSN (Online) 2581-9429
International Journal of Advanced Research in Science, Communication and Technology (IJARSCT)
Volume 11, Issue 1, November 2021
Impact Factor: 5.731

When CNFs@Ni(OH) $_2$ is immersed in $SnCl_4$ aqueous solution, further cation displacement reactions (3) and (4) will occur between Ni(OH) $_2$ and Sn^{4+} ions:

$$Ni(OH)_2 \rightarrow Ni^{2+} + 2OH^- \quad (3)$$

$$Sn^{4+} + 4OH^- \rightarrow Sn(OH)_4 \quad (4)$$

The main driving force from the displacement reaction of Ni (OH) $_2$ and of Sn (OH).$_4$ the difference between the solubility, of Sn (OH) .$_4$ of K SP value (solubility product) of 10×1.0^{-56} , far less than the Ni (OH) The K sp value of 2 is 2.0×10^{-15} , and the smaller the K sp value, the easier the compound exists in the form of precipitation [36] . When the cation displacement reaction occurs, Sn^{4+} replaces part of the Ni $^{2+}$ in the Ni(OH) $_2$ nanoparticles , and Sn(OH) $_4$ precipitates are generated in situ . Under the same conditions of reaction time, the degree of displacement reaction can be controlled by the concentration of Sn^{4+} in the solution. In addition, the ionic radius of Ni $^{2+}$ is 72 pm, and the ionic radius of Sn^{4+} is 71 pm. Because the ionic radius is very close, when the ion exchange reaction occurs between the cations, the product can well retain the fiber structure that the sample had before the replacement. After the sample is calcined at 600 □, the CNFs of the nanofiber skeleton are decomposed, and $Sn(OH)_4$ and Ni(OH) $_2$ are converted into SnO_2 and NiO, respectively , to obtain SnO_2-NiO composite nanofibers.

Figure 3 shows the SEM pictures of SnO_2-NiO-1, SnO_2-NiO-2, SnO_2-NiO-3 and SnO_2-NiO-4 NFs. It can be seen from Figure 3 that the first three samples generally maintain a three-dimensional network structure composed of fibers, and the nanofibers have good continuity and uniformity. After the last sample is heat treated, the nanofibers are broken and the uniformity changes. Difference. From Figure 3 (a), the hollow structure of the SnO_2-NiO-1 NFs sample can be observed. As the concentration of the $SnCl_4$ solution in the substitution reaction increases, more Ni(OH) $_2$ in the sample is replaced with Sn(OH) $_4$, and the fiber diameter of the resulting product is continuously reduced. SnO_2-NiO-1 NFs, SnO The fiber diameters of 2 /NiO-2 NFs and SnO_2 /NiO-3 NFs are 200, 100, and 50 nm, respectively. In the cation replacement process, in order to maintain the charge balance, the replacement of 2 mol Ni $^{2+}$ by 1 mol Sn^{4+} is the main factor that causes the reduction of the fiber diameter of the product.

Table I shows the normalized molar percentages of Ni and Sn elements in each sample. According to Table I, it can be proved that Sn^{4+} and Ni(OH) $_2$ have a cation displacement reaction, and as the displacement reaction progresses, the concentration of Sn^{4+} in the aqueous solution increases, and the relative molar content of Sn in the sample increases. Inferred results are consistent. The experimental results show that the preparation method proposed in this study can be used to control the relative percentage of each component in the SnO_2-NiO composite fiber by adjusting the concentration of the $SnCl_4$ solution in the cation displacement reaction.

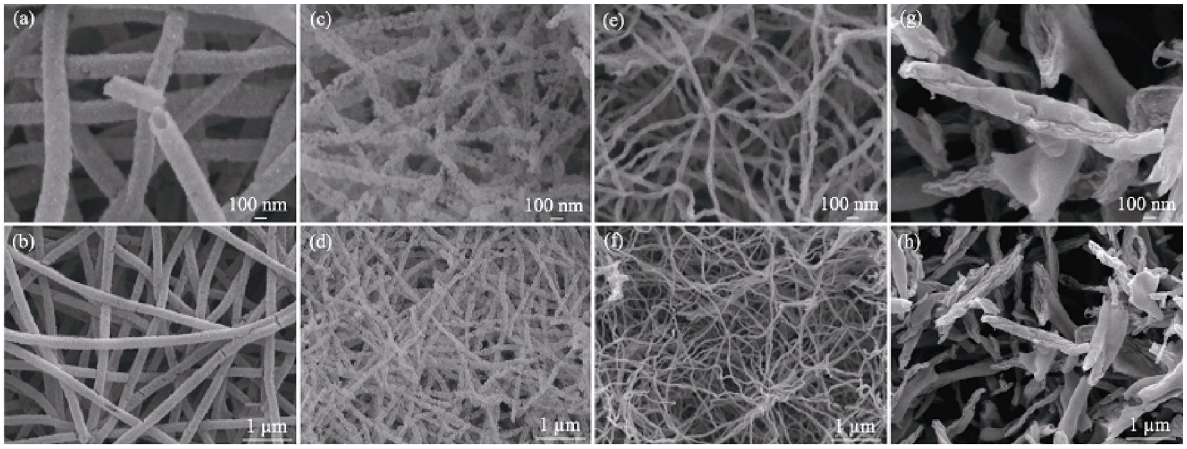

Figure 3: SEM images of **(a, b)**SnO_2 /NiO-1 NFs, **(c, d)**SnO_2 /NiO-2 NFs, **(e, f)**SnO_2 /NiO-3 NFs, and **(g, h)**SnO_2 /NiO-4 NFs

IJARSCT
ISSN (Online) 2581-9429
International Journal of Advanced Research in Science, Communication and Technology (IJARSCT)
Volume 11, Issue 1, November 2021
Impact Factor: 5.731

Table 1: Relative molar percentages of Ni and Sn in NiO NFs and SnO_2 /NiO NFs samples

Sample	Ni/%	Sn/%
NiO NFs	100	0
SnO_2-NiO-1 NFs	76.79	23.21
SnO_2-NiO-2 NFs	25.46	74.54
SnO_2-NiO-3 NFs	0.51	99.49
SnO_2-NiO-4 NFs	0.08	99.92

Figure 4 is the XRD pattern of the SnO_2-NiO composite nanofiber series samples. The sample SnO_2-NiO-1 NFs has obvious diffraction peaks at 2 θ = 37.2°, 43.3° and 62.8°, corresponding to the (111) of NiO. , (200) and (220) crystal planes, which are consistent with the characteristic peak positions of the standard NiO card (PDF 78-0423). No characteristic peak of SnO_2 is detected, indicating that SnO_2-NiO-1 NFs are mainly composed of NiO. 2 The content is very small, and no other impurity peaks are detected. The XRD pattern of the sample SnO_2-NiO-2 NFs showed that it not only contained the characteristic peaks of NiO, but also detected three corresponding to the standard SnO_2 card (PDF 88-0287) at 2 θ = 26.6°, 33.9° and 51.8° The diffraction peak indicates that the sample is composed of NiO and a considerable amount of SnO_2 . The sample SnO_2-NiO-3 NFs showed peaks corresponding to the standard SnO_2 card (PDF88-0287) at 2 θ = 26.6°, 33.9° and 51.8° , and there were no obvious peaks, indicating that the sample is mainly composed of SnO_2 . The content of NiO is very small, which is consistent with the results of EDS analysis. The sample SnO_2XRD pattern of /NiO-4 NFs is similar to the sample SnO_2-NiO-3 NFs, and corresponds to the diffraction peaks of the standard SnO_2 card (PDF 88-0287).

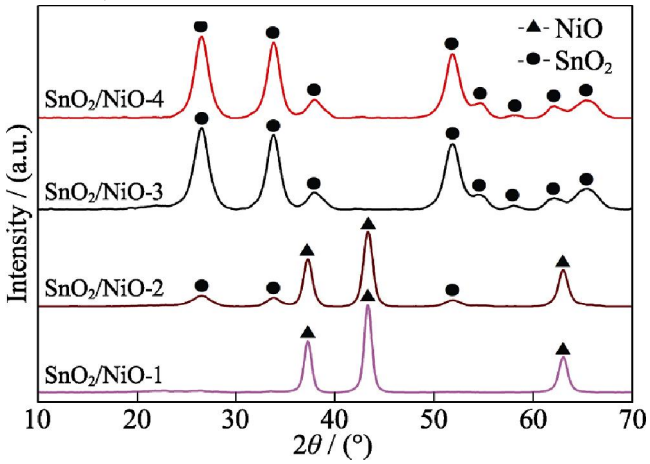

Figure 4: XRD patterns of SnO_2-NiO-1 NFs, SnO_2-NiO-2 NFs,SnO_2-NiO-3 NFs, and SnO_2-NiO-4 NFs

The average grain size of each sample is calculated according to the Scherrer formula:

$$D=K\lambda/\beta\cos\theta \quad (5)$$

Among them, K is the Scherrer constant, K = 0.89; λ is the X-ray wavelength, which is 0.154056 nm; β is the half-height width of the sample diffraction peak, which needs to be converted into radians during the calculation; θ is the Bragg diffraction angle; D is the crystal grain perpendicular to The average thickness in the crystal plane direction, that is, the crystal grain size.

The three strongest characteristic peaks in the XRD pattern of each sample were calculated, and the samples SnO_2-NiO-1 NFs, SnO_2-NiO-2 NFs, SnO_2-NiO-3 NFs, and SnO_2-NiO-4 NFs were obtained. The average grain sizes are 11.1, 7.4, 6.3 and 6.3 nm, respectively.According to the formula of grain boundary density and grain size [37]:

$$\delta=1 / D^2 \quad (6)$$

Among them, δ is the grain boundary density and D is the average grain size. SnO_2-NiO-1 NFs, SnO_2-NiO-2 NFs, SnO_2-NiO-3 NFs and SnO_2-NiO-4 NFs can be calculated . The grain boundary density were 10×8.12^{-9} , 18.46×10^{-9}, 25.16×10^{-9} and 10×25.16^{-9} mm^{-2} , see table II below. Among them, SnO_2-NiO-3 NFs and SnO_2-NiO-4 NFs have

IJARSCT
ISSN (Online) 2581-9429
International Journal of Advanced Research in Science, Communication and Technology (IJARSCT)
Volume 11, Issue 1, November 2021
Impact Factor: 5.731

the smallest grain size and the largest grain boundary density. Grain boundary is a kind of surface defect in solid materials, has high grain boundary energy, and is often the active center for adsorption/desorption of target gas. The activity at the grain boundary is high, the atoms are in an unstable state, and there is an energy level barrier, which has an amplifying effect on the gas sensitivity of the material.

Table 2: Respective grain size (D) and grain boundary density (δ) of SnO_2-NiO NFs samples

Sample	Grain size, D /nm	Grain boundary density, /(×10 ^{9} , mm $^{-2}$)
SnO_2-NiO-1 NFs	11.1	8.12
SnO_2-NiO-2 NFs	7.4	18.46
SnO_2-NiO-3 NFs	6.3	25.16
SnO_2-NiO-4 NFs	6.3	25.16

3.2 Gas Sensitivity Characteristics and Mechanism

The sample was tested for gas sensing, and the gas sensing performance of SnO_2-NiO composite nanofibers was studied. The gas sensing properties of MOS sensing materials are based on the change in resistance caused by the chemical reaction between the adsorbed oxygen on the surface of the material and the target gas. When the gas-sensitive material is in contact with the target gas, the resistance value changes depending on the type of carriers in the material and the properties of the target gas. For n-type semiconductors with electrons as the main carrier, the formation of adsorbed oxygen causes the formation of electron depletion layers (EDLs) on the surface of the material, resulting in an increase in the resistance of the gas-sensitive material. Once the reducing gas is introduced, it will react with the adsorbed oxygen on the surface and at the same time release electrons back to the metal oxide, reducing the resistance of the material. The conduction mechanism of p-type semiconductors is opposite to that of n-type semiconductors. In the air, oxygen is adsorbed on the surface of p-type semiconductor materials to form hole accumulation layers (HALs). The change in the conductivity of the material when in contact with the target gas mainly occurs On the surface of the hole accumulation layer, the change law of resistance in a reducing atmosphere is opposite to that of n-type semiconductors [38,39] . The response sensitivity of the gas-sensitive material to the target gas is determined by the ratio of its resistance in the air (R_a) to the resistance (R_g) in the gas to be measured ($S = R_a / R_g$ or $S = R_g / R_a$) To characterize. For gas-sensitive material in response to a value greater than 1, for the n-type MOS sensitive material, sensitivity with R &lt$_A$ / R &lt$_G$ represents the sensitivity of p-type MOS sensitive material with R &lt$_G$ / R &lt$_A$ represents.

With ethanol gas as the target gas, NiO NFs, SnO_2-NiO-1 NFs, SnO_2-NiO-2 NFs, SnO_2-NiO-3 NFs and SnO_2-NiO-4 NFs were tested at 100~280 □. volume fraction at an operating temperature of 10 × 100 $^{-6}$ response sensitivity curve ethanol gas, the results in Fig. 5 shown in (a). At the optimal working temperature (140 □), the sensitivity of NiO NFs to ethanol gas with a volume fraction of 100×10 $^{-6}$ is 1.6. Among the SnO_2-NiO composite nanofibers, SnO_2-NiO-3 NFs and SnO_2-NiO-4 NFs have better sensitivity, and have better sensitivity to ethanol gas with a volume fraction of 100×10 $^{-6}$ at the optimal working temperature of 160 and 180 □ . The sensitivity reached 13 and 13.4, respectively, which is 8.13 and 8.38 times that of NiO NFs.

Figure 5 (b) shows the volume fraction of NiO NFs, SnO_2-NiO-1 NFs, SnO_2-NiO-2 NFs, SnO_2-NiO-3 NFs, and SnO_2-NiO-4 NFs at their respective optimal working temperatures. 100×10 $^{-6}$The response recovery curve of ethanol gas, in order to facilitate comparison, according to the gas-sensitive response behavior of different materials, the ordinate of the response recovery curve is normalized to obtain the response recovery percentage. When sensitive material behaves as an n-type semiconductor property, response and recovery percentage of | R &lt - R &lt$_A$ | / R &lt$_A$; when the sensitive material behaves as a p-type semiconductor properties, the response recovery percentage (R &lt - R &lt$_A$) / R &lt$_G$. The experimental results show that the samples NiO NFs, SnO_2-NiO-1 NFs and SnO_2-NiO-2 NFs all exhibit the gas-sensing characteristics of p-type semiconductor materials. NiO is a p-type semiconductor material. The main component of SnO_2-NiO-1 NFs and SnO_2-NiO-2 NFs samples is NiO, so the composite fiber exhibits the same p-type semiconductor characteristics as NiO. With the increase of Sn content, SnO_2 gradually becomes the main component in the composite material, and the composite material begins to change from the p-type semiconductor

IJARSCT
ISSN (Online) 2581-9429
International Journal of Advanced Research in Science, Communication and Technology (IJARSCT)
Volume 11, Issue 1, November 2021
Impact Factor: 5.731

sensing characteristics dominated by NiO to the n-type semiconductor sensing characteristics consistent with SnO_2 .SnO_2-NiO-3 NFs and SnO_2-NiO-4 NFs exhibit n-type semiconductor gas-sensing characteristics.

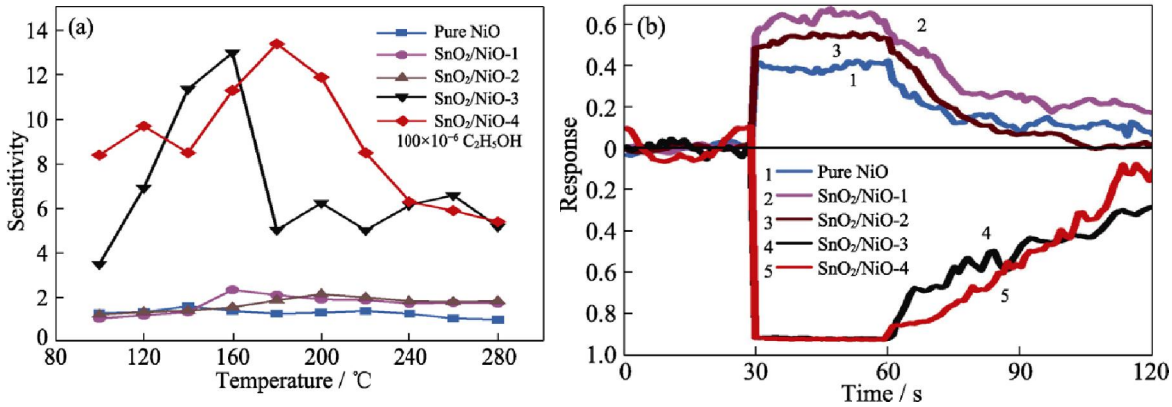

Figure 5: (a) Sensitivity curves of NiO NFs, SnO_2-NiO-1 NFs, SnO_2-NiO-2 NFs, SnO_2-NiO-3 NFs, and SnO_2-NiO-4 NFs to ethanol gas at different temperatures **(b)** response recovery curve to 100×10^{-6} ethanol gas (volume fraction) at the optimal working temperature

The experiment tested NiO NFs, SnO_2-NiO-1 NFs, SnO_2-NiO-2 NFs, SnO_2-NiO-3 NFs, and SnO_2-NiO-4 NFs at their respective optimal working temperatures for a volume fraction of 100×10^{-6} response to different target gases, results in Fig. 6. It can be seen that the response values of SnO_2-NiO-1 NFs and SnO_2-NiO-2 NFs to different gases are relatively low, and the response values of SnO_2-NiO-3 NFs and SnO_2-NiO-4 NFs to different gases are relatively low. It is higher than the sample SnO_2-NiO-1 NFs and SnO_2-NiO-2 NFs. Among them, SnO_2-NiO-3 NFs has the best selectivity to ethanol, and the response value is more than 2.8 times that of other gases; SnO_2-NiO In addition to ethanol, -4 NFs also showed higher response values to acetone and methanol gas.

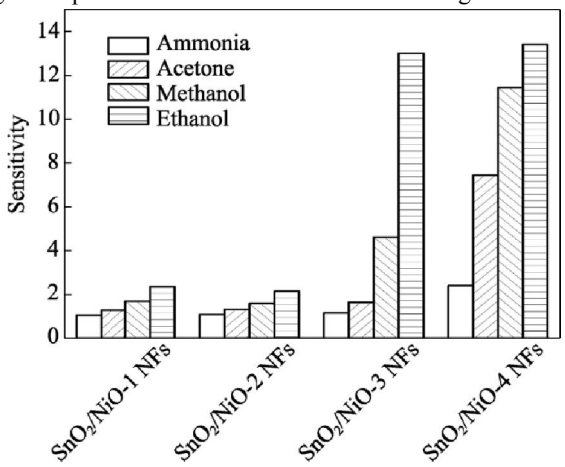

Figure 6: Selectivity of SnO_2-NiO-1 NFs, SnO_2-NiO-2 NFs, SnO_2-NiO-3 NFs, and SnO_2-NiO-4 NFs to various target gases(100 mg/L)

Considering the response sensitivity, working temperature and ethanol selectivity of the SnO_2-NiO composite fiber sample, the SnO_2-NiO-3 NFs sample has the best ethanol gas sensitivity. In order to further explore the practical application performance of SnO_2-NiO-3 NFs in ethanol sensing, under the same test conditions, the ethanol gas sensing performance of SnO_2-NiO-3 NFs and MQ-3 gas sensors was compared and analyzed. The results as Figure 7 (a) is the response sensitivity curve of SnO_2-NiO-3 NFs and MQ-3 to ethanol gas with a volume fraction of 100×10^{-6} at different temperatures. The maximum sensitivity of SnO_2-NiO-3 NFs is 6.17, and the optimal operating temperature of SnO_2-NiO-3 NFs is 160 □, and the maximum sensitivity is 13. It can be seen that, compared with MQ-3, the SnO_2-NiO-3

IJARSCT
ISSN (Online) 2581-9429
International Journal of Advanced Research in Science, Communication and Technology (IJARSCT)
Volume 11, Issue 1, November 2021
Impact Factor: 5.731

NFs sample has higher response sensitivity to ethanol gas, and the optimal working temperature is greatly reduced. When the working temperature of the gas sensitivity test is lower than 280 □, SnO 2 -NiO-3 NFs shows higher sensitivity than MQ-3. Figure 7 (b) is the response recovery curve of sample SnO 2 -NiO-3 NFs and MQ-3 to ethanol gas with a volume fraction of 100×10^{-6} at the optimal working temperature. The recovery time of NiO-3 NFs is longer than that of MQ-3, and the response recovery curve of MQ-3 is smoother, indicating that the MQ-3 gas sensor has better stability. Through comparison, it can be seen that the sample SnO_2-NiO-3 NFs not only has a significant increase in sensitivity, but also has a low operating temperature, which reduces the energy consumption of the sensor and has good practical application value as a gas-sensitive material.

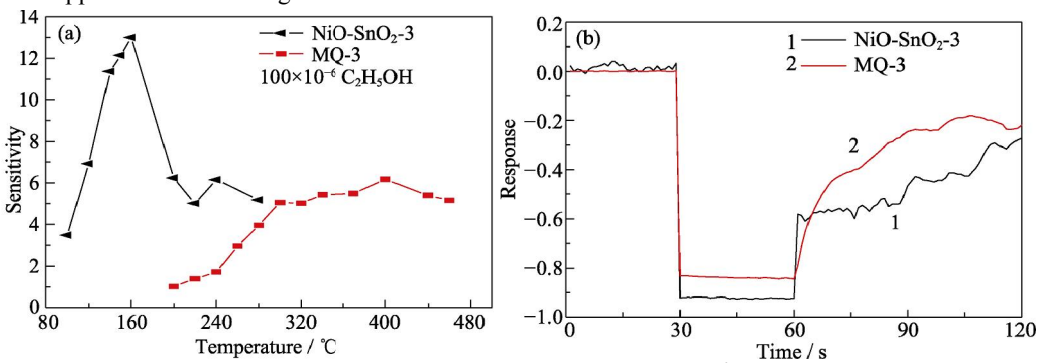

Figure 7: (a) Sensitivity curves of SnO_2-NiO-3 NFs and MQ-3 to 100×10^{-6} ethanol gas at different working temperatures, and **(b)** response recovery curve to 100×10^{-6} ethanol gas at the optimal working temperature

Table III compares the ethanol sensing characteristics of the experimental sample SnO_2-NiO-3 NFs and some SnO_2 based sensors reported in the literature. It can be seen that SnO_2-NiO-3 NFs is at a lower working temperature (160 □). Bottom, it has relatively considerable gas response sensitivity. A lower working temperature is more conducive to improving the response stability of the sensor and prolonging the service life of the sensor.

Table 3: Comparison of the characteristics of some SnO2 -based ethanol sensors reported in the literature with this work

Materials	Temperature/□	Response/(100 mg·L^{-1})	Ref.
Hierarchical SnO_2	300	24.1	[40]
ZnO-SnO_2 nanofibers	300	18.0	[41]
Horseshoe-shaped SnO_2	225	17.3	[42]
NiO-decorated SnO_2nanorods	300	30.0	[43]
SnO_2-NiO composite nanofibers	160	13.0	This work

According to the sensing mechanism of MOS gas-sensitive materials, the gas-sensitive performance of MOS is closely related to factors such as the composition, surface state and morphology, and operating temperature of the material [44]. The gas sensitivity test shows that the sample SnO_2 /NiO-3 NFs shows good gas sensitivity to ethanol gas. Compared with the common MQ-3 gas sensor on the market, the working temperature is lower and the sensitivity is higher. The unique shape is related to the composition.SnO_2 is a typical n-type semiconductor material, and the main carriers are electrons. When the sensor material is exposed to air, the oxygen adsorbed on the surface of the material and is O - (experimental work temperature 90 ~ 280 □) present in the form [45, 46] , the adsorbed oxygen grab some electronic sensing material, a carrier The electron concentration of the ions decreases, and the resistance increases (Equation (7)). When the sensing material is exposed to ethanol gas, the ethanol gas will undergo an oxidation-reduction reaction with the O - ions on the surface of the material, and the captured electrons will be released back into the material (Equation (8)). At this time, the electron consumption of SnO_2 The final layer becomes thinner and the resistance decreases [33, 47].

$$O_2(g)+2e^-\rightarrow 2O^-(abs) \quad (7)$$

$$C_2H_5OH(g)+6O-(abs)\rightarrow 2CO_2(g)+3H_2O(g)+6e^- \quad (8)$$

IJARSCT
ISSN (Online) 2581-9429
International Journal of Advanced Research in Science, Communication and Technology (IJARSCT)
Volume 11, Issue 1, November 2021
Impact Factor: 5.731

In terms of morphology, SnO_2-NiO-3 NFs retains the unique nanofiber network structure of electrospinning, and has a large adsorption area, which provides a channel for the diffusion of the target gas in the material. The nanofiber structure can effectively inhibit the agglomeration of metal oxide particles during the heat treatment process, and the fiber structure can also promote carrier transport. These are important factors to improve the gas sensitivity of the sample [32]. In terms of structure, due to the similar size of Ni^{2+} (ionic radius of 72 pm) and Sn^{4+} (ionic radius of 71 pm), Ni^{2+} ions can enter the SnO_2 lattice to replace Sn^{4+} and occupy Sn^{4+} The original location. When Ni^{2+} replaces Sn^{4+} ions, the electron concentration will decrease to compensate for the local charge, and the defect reaction that occurs at this time is shown in equation (9) [48].

$$NiO+2e^{/}\rightarrow SnO_2Ni_{Sn}^{//}+O_O^X+V_O^X \quad (9)$$

When SnO_2 is doped with Ni ions, the electron density of the material decreases and the concentration of oxygen vacancies increases. Oxygen vacancies are often the active centers for reactions on the surface of the material. The progress of reaction (9) enhances the oxygen adsorption and ionization capabilities of the SnO_2 surface, and plays a positive role in improving the gas sensitivity of the sensing material, and at the same time reduces the electron density on the surface of the material, so that the surface can absorb more oxygen. , resulting in the electron depletion layer thicker, R & it is increased, thus contributing to improving the sensitivity of the n-type semiconductor material. In summary, the addition of Ni can improve the adsorption and ionization capacity of oxygen on the surface of SnO_2 , which is beneficial to the improvement of the gas sensitivity of the material.

IV. Conclusion

NiO NFs with hollow nanofiber structure were prepared by electrospinning, chemical precipitation reaction and heat treatment. Sn element was introduced into NiO through ion displacement reaction, and SnO_2-NiO composite fiber materials with different SnO_2 content were prepared, and the gas sensitivity performance test and analysis of the composite materials were carried out with ethanol as the target gas. The results show that the addition of SnO_2 improves the gas sensitivity of NiO nanofibers to ethanol gas. Among them , the selectivity of SnO_2-NiO-3 NFs is better, the working temperature is lower, and the optimum working temperature is 160 ◎ for 100×10^{-6} The sensitivity of ethanol gas reaches 13. Compared with the common SnO_2 based gas sensor element MQ-3 on the market, SnO_2-NiO-3 NFs have higher response sensitivity and lower working temperature. The preparation method of SnO_2-NiO-3 NFs is simple, and the structure is flexible. It has certain practical application value in the sensor of ethanol gas.

References

[1]. YAMAZOE NOBORU, SHIMANOE KENGO. Receptor function and response of semiconductor gas sensor, Journal of Sensors ,2009, 2009:875704.

[2]. BARSAN N, KOZIEJ D, WEIMAR U. Metal oxide-based gas sensor research: How to?, Sensors and Actuators B: Chemical ,2007, 121(1):18-35.

[3]. MORAN-LAZARO J P, GUILLEN-LOPEZ E S, LOPEZ-URIAS F, et al. Synthesis of ZnMn2 O 4 nanoparticles by a microwave-assisted colloidal method and their evaluation as a gas sensor of propane and carbon monoxide, Sensors ,2018, 18(3):701.

[4]. LEE JEONGSEOK, LEE SE-HYEONG, BAK SO-YOUNG, et al. Improved sensitivity of α -Fe 2 O 3 nanoparticle-decorated ZnO nanowire gas sensor for CO, Sensors ,2019, 19(8):1903.

[5]. WANG XU, LI SIHAN, XIE LILI, et al. Low-temperature and highly sensitivity H 2 S gas sensor based on ZnO/CuO composite derived from bimetal metal-organic frameworks, Ceramics International ,2020, 46(10):15858-15866.

[6]. LEONARDI S G, MIRZAEI A, BONAVITA A, et al. A comparison of the ethanol sensing properties of alpha-iron oxide nanostructures prepared via the Sol-Gel and electrospinning techniques,Nanotechnology ,2016, 27(7):075502.

[7]. MIRZAEI ALI, PARK SUNGHOON, SUN GUN-JOO, et al. Fe 2 O 3 /Co 3 O 4 composite nanoparticle ethanol sensor,Journal of the Korean Physical Society ,2016, 69(3):373-380.

IJARSCT
ISSN (Online) 2581-9429
International Journal of Advanced Research in Science, Communication and Technology (IJARSCT)
Volume 11, Issue 1, November 2021
Impact Factor: 5.731

[8]. CHOI SEUNGBOK, BONYANI MARYAM, SUN GUN-JOO, et al. Cr 2 O 3 nanoparticle-functionalized WO 3 nanorods for ethanol gas sensors,Applied Surface Science ,2018, 432:241-249.

[9]. ZHOU XINYUAN, WANG YING, WANG JINXIAO, et al. Amplifying the signal of metal oxide gas sensors for low concentration gas detection,IEEE Sensors Journal ,2017, 17(9):2841-2847.

[10]. HU WEIYE. Vehicle alcohol detection system based on Internet of things technology,IOP Conference Series: Materials Science and Engineering ,2018, 452:042156.

[11]. WEI BEE-YU, HSU MING-CHIH, SU PI-GUEY, et al. A novel SnO2 gas sensor doped with carbon nanotubes operating at room temperature, Sensors and Actuators B: Chemical ,2004, 101(1/2):81-89.

[12]. SHARMA HEMLATA JAYPRAKSH, SONWANE NAYANA DAMODHAR, KONDAWAR SUBHASH BABURAO. ElectrospunSnO2 /polyaniline composite nanofibers based low temperature hydrogen gas sensor, Fibers and Polymers ,2015, 16(7):1527-1532.

[13]. CHO SOO-YEON, YOO HAE-WOOK, KIM JU YE, et al. High-resolution p-type metal oxide semiconductor nanowire array as an ultrasensitive sensor for volatile organic compounds, Nano Letters ,2016, 16(7):4508-4515.

[14]. MOON YOUNG KOOK, JEONG SEONG-YONG, KANG YUN CHAN, et al. Metal oxide gas sensors with Au nanocluster catalytic overlayer: Toward tuning gas selectivity and response using a novel bilayer sensor design,ACS Applied Materials Interfaces ,2019, 11(35):32169-32177.

[15]. AMIRI VAHID, ROSHAN HOSSEIN, MIRZAEI ALI, et al. Nanostructured metal oxide-based acetone gas sensors: a review,Sensors ,2020, 20(11):3096.

[16]. NUNDY SRIJITA, EOM TAE-YIL, KANG JUN-GU, et al. Flower-shaped ZnOnanomaterials for low-temperature operations in NO X gas sensors,Ceramics International ,2020, 46(5):5706-5714.

[17]. SHAALAN N M, YAMAZAKI T, KIKUTA T, et al. Influence of morphology and structure geometry on NO 2 gas-sensing characteristics of SnO 2 nanostructures synthesized via a thermal evaporation method,Sensors and Actuators B: Chemical ,2011, 153(1):11-16.

[18]. GAIDAN IBRAHIM, ASBIA SALIM, BRABAZON DERMOT, et al. TiO2 gas sensor to detect the propanol at room temperature,AIP Conference Proceedings ,2017, 1896(1):1-5.

[19]. YAN SHUANG, WU QINGSHENG. A novel structure for enhancing the sensitivity of gas sensors- α -Fe 2 O 3 nanoropes containing a large amount of grain boundaries and their excellent ethanol sensing performance,Journal of Materials Chemistry A ,2015, 3(11):5982-5990.

[20]. ZHANG JIAN, ZENG DAWEN, ZHU QIANG, et al. Effect of grain-boundaries in NiOnanosheet layers room-temperature sensing mechanism under NO 2, Journal of Physical Chemistry C ,2015, 119(31):17,930-17,939.

[21]. TURGUT ERDAL, COBAN OMER, SARITAS SEVDA, et al. Oxygen partial pressure effects on the RF sputtered p-type NiO hydrogen gas sensors,Applied Surface Science ,2018, 435:880-885.

[22]. ZENG QINGHAO, CUI YANFA, ZHU LIANFENG, et al. Increasing oxygen vacancies at room temperature in SnO2 for enhancing ethanol gas sensing,Materials Science in Semiconductor Processing ,2020, 111:104962.

[23]. LI XIN, ZHANG HANG, FENG CHANGHAO, et al. Novel cage-like α -Fe 2 O 3 /SnO2 composite nanofibers by electrospinning for rapid gas sensing properties, RSC Advanced. ,2014, 4(52):27552-27555.

[24]. JAYABABU NAGABANDI, POLOJU MADHUKAR, SHRUTHI JULAKANTI, et al. Semi shield driven pnheterostructures and their role in enhancing the room temperature ethanol gas sensing performance of NiO/SnO2nanocomposites, Ceramics International ,2019, 45(12):15134-15142.

[25]. WEI ZHIJIE, ZHOU QU, WANG JINGXUAN, et al. Hydrothermal synthesis of SnO2nanoneedle-anchored NiO microsphere and its gas sensing performances, Nanomaterials ,2019, 9(7):1015.

[26]. GUO JING, ZHANG JUN, ZHU MIN, et al. High-performance gas sensor based on ZnO nanowires functionalized by Au nanoparticles, Sensors and Actuators B: Chemical ,2014, 199:339-345.

IJARSCT
ISSN (Online) 2581-9429
International Journal of Advanced Research in Science, Communication and Technology (IJARSCT)
Volume 11, Issue 1, November 2021
Impact Factor: 5.731

[27]. LONG JING, XIONG WEI, WEI CHENGYIRAN, et al. Directional assembly of ZnO nanowires via three-dimensional laser direct writing, Nano Letters ,2020, 20(7):5159-5166.

[28]. LIU BILU, LIU QINGFENG, REN WENCAI, et al. Synthesis of single-walled carbon nanotubes, their ropes and books,ComptesRendus Physique ,2010, 11(5/6):349-354.

[29]. SCHOTTLE MARIUS, XIA QINGBO, CHENG YEN THENG, et al. Integrated polyphenol-based hydrogel templating method for functional and structured oxidicnanomaterials,Chemistry of Materials ,2020, 32(11):4716-4723.

[30]. LIU ZICHEN, MURPHY ALEXANDER WILLIAM ALLEN, KUPPE CHRISTIAN, et al. WS 2 nanotubes, 2D nanomeshes, and 2D in-plane films through one single chemical vapor deposition route,ACS Nano ,2019, 13(4):3896-3909.

[31]. BAI SHOULI, GUO WENTAO, SUN JIANHUA, et al. Synthesis of SnO 2 -CuOheterojunction using electrospinning and application in detecting of CO,Sensors and Actuators B: Chemical ,2016, 226:96-103.

[32]. YAN SHUANG, WU QINGSHENG. MicroporedSn-SnO 2 /carbon heterostructure nanofibers and their highly sensitive and selective C 2 H 5 OH gas sensing performance,Sensors and Actuators B: Chemical ,2014, 205:329-337.

[33]. DONG SHUWEN, WU DI, GAO WENYUAN, et al. Multi- dimensional templated synthesis of hierarchical Fe 2 O 3 /NiO composites and their superior ethanol sensing properties promoted by nanoscalepnheterojunctions, Dalton Transitions ,2020, 49(4):1300-1310.

[34]. RHEINGANS BASTIAN, MITTEMEIJER ERIC J. Modelling precipitation kinetics: evaluation of the thermodynamics of nucleation and growth,Calphad ,2015, 50:49-58.

[35]. LI LU, BAO ZHILONG, YE XUNHENG, et al. Nucleation, growth, and aggregation of Au nanocrystals on liquid surfaces,Chinese Physics Letters ,2020, 37(2):028102.

[36]. WANG XIAOMING, PHILLIPS BRIAN L, BOILY JEAN-FRANCOIS, et al. Phosphate sorption speciation and precipitation mechanisms on amorphous aluminum hydroxide, Soil Systems ,2019, 3(1):20.

[37]. AYED RIHAB BEN, AJILI MEJDA, GARCIA JORGE M, et al. Physical properties investigation and gas sensing mechanism of Al: Fe 2 O 3 thin films deposited by spray pyrolysis, Superlattices and Microstructures ,2019, 129:91-104.

[38]. MIRZAEI ALI, LEE JAE-HYOUNG, MAJHI SANJIT MANOHAR, et al. Resistive gas sensors based on metal-oxide nanowires, Journal of Applied Physics ,2019, 126(twenty four):241102.

[39]. GUMBI SIFISO W, MKWAE PRINCE S, KORTIDIS IOANNIS, et al. Electronic and simple oscillatory conduction in ferrite gas sensors: gas-sensing mechanisms, long-term gas monitoring, heat transfer, and other anomalies, ACS Applied Materiale Interfaces ,2020, 12(38):43231-43249.

[40]. ZHOU XIAOMING, FU WUYOU, YANG HAIBIN, et al. Novel SnO2 hierarchical nanostructures: synthesis and their gas sensing properties,Materials Letters ,2013, 90(1):53-55.

[41]. SONG XIAOFENG, LIU LI. Characterization of electrospunZnO-SnO2 nanofibers for ethanol sensor, Sensors & Actuators A Physical ,2009, 154(1):175-179.

[42]. LU GEYU, ZHANG BO, SUN YANGFENG, et al. Horseshoe-shaped SnO2 with annulus-like mesoporousforethanol gas sensing application, Sensors & Actuators B Chemical ,2017, 240:1321-1329.

[43]. SUN GUN-JOO, LEE JAE KYUNG, LEE WAN IN, et al. Ethanol sensing properties and dominant sensing mechanism of NiO-decorated SnO 2 nanorod sensors, Electronic Materials Letters ,2017, 13(3):260-269.

[44]. DEY ANANYA. Semiconductor metal oxide gas sensors: a review, Materials Science and Engineering: B ,2018, 229:206-217.

[45]. BARSAN NICOLAE, WEIMAR UDO. Conduction model of metal oxide gas sensors, Journal of Electroceramics ,2001, 7(3):143-167.

[46]. GAO HONGYU, YU QI, ZHANG SUFANG, et al. Nanosheet- assembled NiO microspheres modified by Sn 2 + ions isovalent interstitial doping for xylene gas sensors, Sensors and Actuators B: Chemical ,2018, 269:210-222.

IJARSCT
ISSN (Online) 2581-9429
International Journal of Advanced Research in Science, Communication and Technology (IJARSCT)
Volume 11, Issue 1, November 2021
Impact Factor: 5.731

[47]. HAO PEI, QIU GE, SONG PENG, et al. Construction of porous LaFeO3 microspheres decorated with NiOnanosheets for high response ethanol gas sensors, Applied Surface Science,2020, 515:146025.

[48]. LI ZHOU, YI JIANXIN. Enhanced ethanol sensing of Ni-doped SnO2 hollow spheres synthesized by a one-pot hydrothermal method, Sensors and Actuators B: Chemical,2017, 243:96-103.